Estimating Material Deformation Characteristics During Orthogonal Cutting Using Digital Image Correlation

Varun Raizada[1], Manjesh Singh[2] and Mohit Law[1,*]

[1] Machine Tool Dynamics Laboratory, Department of Mechanical Engineering, Indian Institute of Technology Kanpur, Kanpur - 208016, India
[2] Department of Mechanical Engineering, Indian Institute of Technology Kanpur, Kanpur - 208016, India
*mlaw@iitk.ac.in

Abstract. During machining, material shears at strains and strain rates that are of several orders of magnitude higher than what the same material would have experienced during typical tensile experiments. Since deformation mechanisms are fundamental to how the material will behave during its manufacture and use in an application, characterizing deformation behavior is essential to develop flow stress and damage models that could be used for predictive purposes. This is only possible by visualizing the machining process using vision-based in-situ monitoring. This paper discusses a framework in which we use a digital image correlation scheme to estimate flow behavior from video of a cutting process. We illustrate the method on video of orthogonal cutting of a hard plastic material with different cutting conditions. We discuss the noise floor and sensitivity of the estimates to image processing and acquisition parameters. We benchmark estimations from video with classical theoretical models. Direct estimates of shear angles are found to agree with model predictions. Estimates for strain rates are observed to increase with cutting velocity whereas indirect estimates for friction are observed to reduce with speed. Since estimates follow expected trends, our framework provides a blueprint for vision-based in-situ characterization of material deformation during machining processes.

Keywords: Machining, Material Deformation, Strain, Strain rate, Digital image correlation.

1 Introduction

Materials deform with high strain (~10^1) and strain rates (~10^5 s^{-1}) during machining. Usual tensile tests are inadequate (very low strain (~10^{-2}) and strain rates (~10^{-3} s^{-1})) to characterize deformation experienced during machining. Since deformation mechanisms are fundamental to how the material will behave during its manufacture and use in an application, characterizing how the material deforms and at the rates it deforms at is essential to develop flow stress and damage models that could be used for predictive purposes. This is only possible by visualizing the machining process using vision-based in-situ monitoring. Presenting such a framework to estimate flow behavior from video of a cutting process is the main scientific aim of this paper.

Previous other research [1 - 7] on using vision for in-situ monitoring of deformations in machining processes included characterizing the influence of tool geometry on chip formation, crack propagation, flow stability, plasticity, shear banding, strain, strain rate, and friction. Most of that work used particle image velocimetry (PIV) and/or digital image correlation (DIC) to estimate deformations in the primary and secondary shearing zones. This was done by cross-correlating groups of speckle particles on the workpiece surface to obtain material displacements and deformations. Most of the prior work was related to monitoring an orthogonal cutting process.

Though prior related research is exemplary and has guiding significance for our own work reported in this paper, prior research did not systematically discuss the noise floor in measurements, and nor did it systematically discuss how estimates for flow behavior are influenced by the DIC parameters or by acquisition parameters. It is hence the explicit aim of this paper to discuss the noise floor and sensitivity of estimates to the interrogation subset size used for cross-correlation and to the subset strain radius. This sensitivity analysis may be considered to be our modest new contribution to the state-of-the-art.

We illustrate estimation of material deformation parameters on video of orthogonal cutting of a hard plastic material. To record high-speed video with high resolutions to result in smaller pixels, we leverage learnings from our related work on methods to estimate small and subpixel level motion from video [8 - 11]. For DIC, we use a MATLAB-based open-source code called Ncorr [12]. We benchmark estimations of shear angles from video with the classical Merchant's theoretical model [13].

The remainder of the paper is organized as follows: first, in Section 2, we present the experimental setup. Section 3 discusses the use of Ncorr and sensitivity of results to DIC parameters. Sections 4 and 5 discuss the main results. The conclusions follow.

2 Experimental Setup

We cut a hard-plastic material with a mild steel tool. The setup for this is shown in Fig. 1(a). The setup was made to mimic a pseudo-orthogonal cutting process. A relatively sharp tool with a rake and clearance angle of 10^{o} each was mounted in a milling holder mounted in a CNC vertical milling machine. The spindle was locked, and the workpiece mounted in a vice was moved relative to the tool at different feed speeds. The width of the tool was greater than the width of the workpiece being cut such as to avoid side spreading of the material and maintain a plain strain condition. No additional constraint was used to prevent out-of-plane flow of material. The depth of the cut was kept fixed at 0.5 mm. A Chronos 2.1 high-speed camera was used to record video of the cutting process at rates of 1000 frames per second. This speed of recording is thought to be sufficient for monitoring the process when material is being cut at speeds of 1.5 m/min, 2 m/min, and 2.5 m/min, respectively. Though these cutting speeds are low, and not typical of cutting speeds in metals, since the aim of this paper is only to establish the framework for characterizing material deformation during machining, the low cutting speeds are deemed acceptable. To achieve the necessary magnification for accurate analysis, a reverse ring was used in conjunction with a Canon 18-55 mm camera lens, connected to the camera via an EIS-C adapter. A DC light was used for illumination. Tool and workpiece were sprayed to establish a speckle pattern that is necessary for DIC.

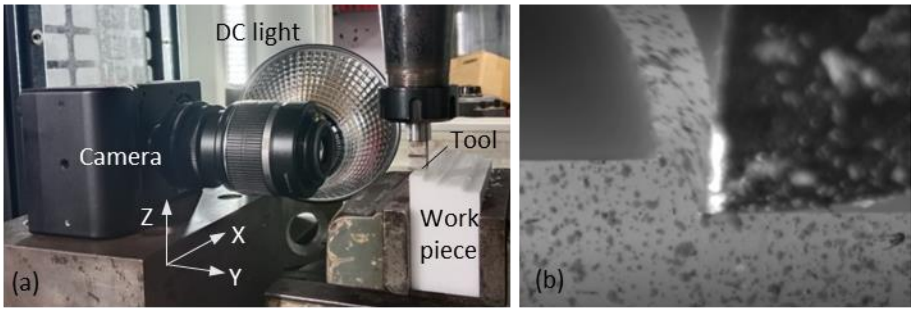

Fig. 1 (a) Experimental setup for vision-based in-situ characterization of material deformation in orthogonal cutting, (b) Representative example of a frame from video.

A typical frame from the video is shown in Fig. 1(b). From images like this, we estimate the deformation field and the shear strains using DIC. Since the frame rate of video recordings is known, we use that information along with the estimated strains to evaluate strain rates. We investigate the influence of DIC parameters on the results including establishing baselines of noise in the measurements, as is discussed in Section 3. From video of the process, we also estimate the deformed chip thickness, from which we estimate the chip thickness ratio and use that in turn to estimate the shear angle from orthogonal theory. We also directly estimate the shear angle from images – as is discussed in Section 4. Using these shear angles, and Merchant's minimum energy principle, we also estimate the friction angle, from which we estimate the coefficient of friction – as is also discussed in Section 4.

3 Sensitivity Analysis using DIC

We discuss herein the noise floor of estimates from DIC and also discuss the sensitivity of estimates to changes in interrogation windows for cross-correlation and to the size of the strain subset radius. We also discuss the influence of rates of image acquisition on the estimated displacements, strains, and strain rates.

3.1 Noise Floor

To trust DIC's ability to resolve motion and estimate strains and strain rates from that motion, we first estimate the noise in the measurements. The main motive of doing so is to be able to distinguish between displacements of material points and noise. The threshold we thus estimate is termed as the noise floor. To estimate this noise floor, we use a video recording of the tool and workpiece when there was no relative movement between them. Since there is no motion, there should be no change of pixel intensities between frames, and as such the resulting displacements obtained with DIC should be zero. To estimate the noise floor, we track a defined region of interest on the tool and partially formed chip, as illustrated in Fig. 2.

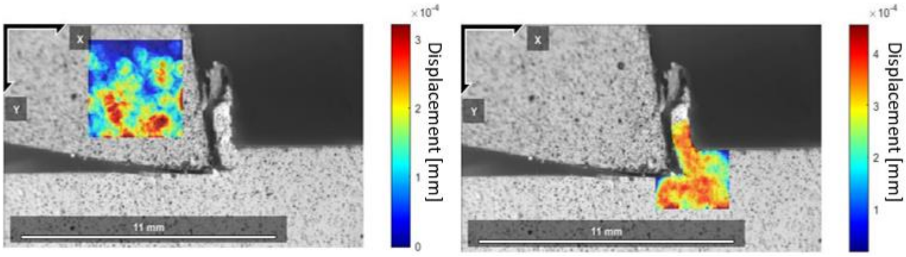

Fig. 2 Representative X-directional displacements of the tool (on the left) and of the workpiece (on the right) estimated by DIC to establish the noise floor. The x-y coordinates shown on the figures are local to the frame and are not related to the machine's axes.

As is evident from the deformation fields and the color bars that represent displacements in Fig. 2, when there is no relative motion between the tool and the workpiece, the X-directional displacements for the tool and workpiece are estimated to be of the order ~10^{-4} mm. This is taken to be noise floor, i.e., for us to be able to obtain reliable results from our analysis, the motion between the reference and current frames must be at least an order of magnitude greater than this for us to be able to distinguish actual motion from noise.

3.2 Influence of the Size of the Interrogation Window

In this section, we discuss the influence of the size of the interrogation window on estimates for displacements. The size of the interrogation window is governed by the radius of the subset between a pair of images that is to be cross correlated. This subset radius from within the primary shearing and deformation zone is shown in Fig. 3. To investigate the influence of the subset radius on displacements, we analyzed results with three different radii: 20 pixels, 40 pixels, and 60 pixels.

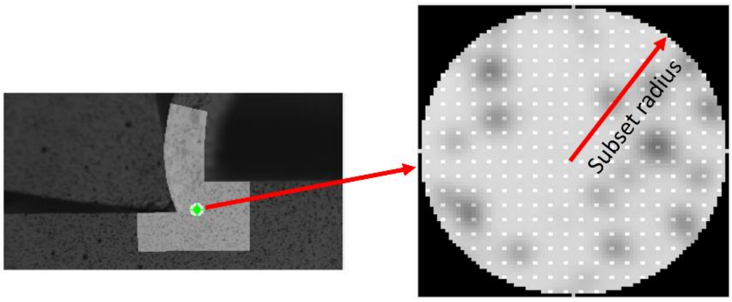

Fig. 3 Subset radius to be cross correlated for estimating displacements.

Our analysis showed that varying the subset size from 20 to 40 to 60 pixels does not significantly influence the calculated displacement or strains estimated from those displacements. However, since larger radii smoothens the gradients at the boundaries, we recommend that large subset radii should be avoided. Likewise, since the interrogation window within smaller radii might not have enough speckles within them to be cross correlated, results with small radii could be misleading. As such, small subset radii too should be avoided. Since small and large subset radii should be avoided, for all further analysis we choose a subset radius of 40 pixels.

3.3 Influence of the Subset Strain Radius

Since strain is calculated by fitting a plane over a displacement field [12], the region of displacements that are to be used for that fitting must be defined a priori. This region is selected by the number of pixels within a certain subset, called the subset strain radius. To investigate the influence of different strain subset radii on the estimated strains, we choose three circles within the primary shearing zone of radii of 5 pixels, 15 pixels, and 25 pixels, respectively. A representative example of such a strain subset radius and the fitted plane is shown in Fig. 4.

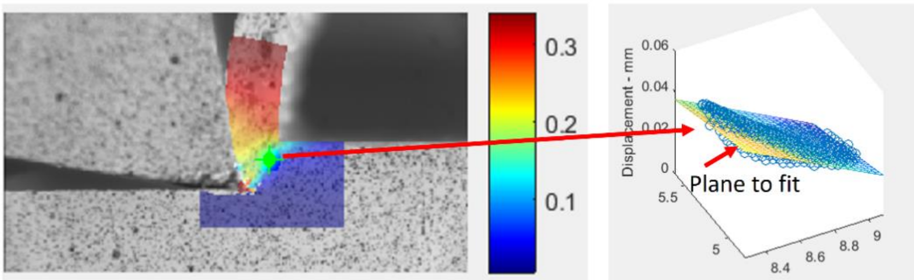

Fig. 4 Fitting a plane over a subset of obtained displacements for strain calculations.

We observed that the estimated strains change with the size of the strain subset radius. We find that a smaller radius typically produces a more accurate local fit, but amplifies noise, whereas increasing the strain subset radius results in a smoother strain field, but with lower strain values. To avoid noise amplification or unwanted smoothing, we conclude that the strain subset radii should be selected based on goodness of fit of the plane over the displacement field, and as such, it is advisable to use the largest possible window that produces a good fit. We hence select the strain subset radii of 15 pixels for all subsequent analysis.

3.4 Influence of the Reference Frame

This section discusses how the selection of the frame of reference may affect the results. Displacement varies from frame to frame, as does the calculated strain. To demonstrate how strain varies with the choice of the reference frame, consider three cases: the first of which uses frame 1 as the reference and frame 5 as the current frame; a second case that uses frame 1 as the reference and frame 2 as the current frame; and lastly, using frame 4 as the reference and frame 5 as the current frame. We observe that displacements decrease by roughly a factor of four when the reference frame and current frame differ by a single frame, compared to a difference of four frames. Similar trends were observed for estimates of strains. Since these results will change with changing framerates, it suggests that since strains depend on the choice of image pairs used for estimating displacements, perhaps a better metric to estimate deformations is strain rate. Estimations of strain rates will be independent of the choice of image pairs and framerates at which the video is recorded. The only constraint on proper estimation of strain rates at higher framerates is that the displacements between a pair of images must be greater than the noise floor.

Having characterized the noise floor and the influence of DIC and acquisition parameters on the results, the next section discusses estimates of orthogonal cutting parameters from images followed by discussions on estimates of strain rates.

4 Estimating Orthogonal Parameters from Video

We discuss herein orthogonal parameters evaluated from video of the cutting process. We evaluate the shear angle (ϕ_c) by two methods. The first is a direct measurement by drawing a line to pass through the region within the primary shear zone that has the highest estimated deformation – shown in Fig. 5 for a representative case. The second method is an indirect one that uses the measured cut chip thickness (h_c) at a suitable section on the rake face – shown also in Fig. 5. In the second method, the measured chip thickness is used along with knowledge of the uncut chip thickness (h) and the rake angle and the geometric relationship between these to estimate the shear angle as:

$$\phi_\mathrm{c} = \tan^{-1}\left(\frac{r_\mathrm{c}\cos\alpha_\mathrm{r}}{1 - r_\mathrm{c}\sin\alpha_\mathrm{r}}\right) \tag{1}$$

wherein r_c is the chip thickness ratio, i.e., the ratio of the uncut chip thickness to the cut chip thickness, and α_r is the rake angle.

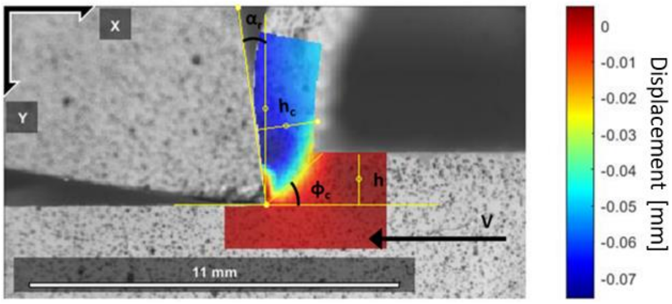

Fig. 5 Orthogonal cutting geometry as observed from the video. The x-y coordinates shown on the figures are local to the frame and are not related to the machine's axes.

Using the estimated shear angles, and taking Merchant's minimum energy principle to be valid for these orthogonal cutting experiments, we also estimate the friction angle, β_{a} from the following relationship:

$$\phi_{\mathrm{c}} = \frac{\pi}{4} - \frac{(\beta_{\mathrm{a}} - \alpha_{\mathrm{r}})}{2}. \quad (2)$$

From the estimated friction angle, the coefficient of friction in turn is estimated as

$$\mu_{\mathrm{a}} = \tan \beta_{\mathrm{a}}. \quad (3)$$

Estimated parameters are listed in Table 1. As is evident, shear angles estimated using both methods broadly agree with each other, and exhibit rate dependency. Friction too shows rate dependency, decreasing with increasing speeds. This is along expected lines, since as speed increases, as does temperature in the cutting region, allowing for easy sliding of the chip on the rake face and reducing friction.

For the higher cutting speed case, the shear angles using both methods are estimated to be greater than 45º. This could be because of errors in measurement of the cut chip thickness, or due to the approximate method of drawing a line through the primary deformation zone which has some finite width, and as such is not a plane. The shear angle being greater than 45º could also be due to the hard-plastic material that we cut exhibiting different plasticity characteristics than what is otherwise typically observed in metals. Nevertheless, since estimating the shear angle and friction coefficient from video of the process is simpler than the manual method of doing so, vision-based methods offer promise.

Table 1. Orthogonal cutting parameters evaluated from video.

Cutting speed [m/min]	Depth of cut [mm]	Direct estimate of shear angle [º]	Indirect estimate of shear angle [º]	Coefficient of friction
1.5	0.5	44.6	42.5	0.18
2	0.5	44.6	43.7	0.18
2.5	0.5	47.5	45.2	0.13

5 Estimating Strains and Strain Rates from Video

We discuss herein the main results related to estimation of strains and strain rates from video of the cutting process. As a representative case for cutting at a speed of 1.5 m/min, the displacements in the *u* and *v* directions are shown in Fig. 6(a) and Fig. 6(b), respectively, and the shear strains ($\in_{\mathrm{xy}}$) are shown in Fig. 6(c). From these estimated shear strains and using the known framerate of video recordings, the shear strain rates ($\dot{\in}_{\mathrm{xy}}$) are estimated. These results are summarized in Table 2, which only lists the maximum $\in_{\mathrm{xy}}$ and $\dot{\in}_{\mathrm{xy}}$ for all experiments. And, though we do not trust the estimates for $\in_{\mathrm{xy}}$ due to their framerate dependency, those are still listed for the sake of completeness.

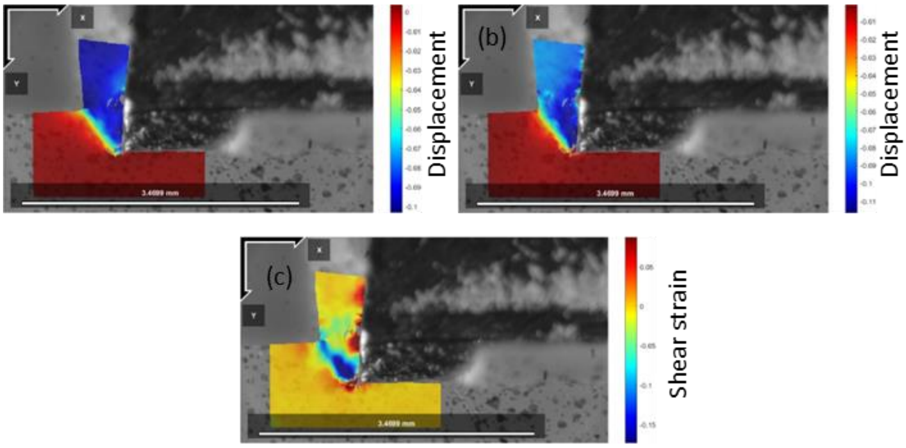

Fig. 6 (a) u (x) and (b) v (y) directional displacements, (c) shear strains for the representative cutting case at a speed of 1.5 m/min. The x-y coordinates shown on the figures are local to the frame and are not related to the machine's axes.

Table 2. Estimated shear strains and shear strain rates.

Cutting speed [m/min]	Depth of cut [mm]	Maximum shear strain (ϵ_{xy})	Maximum shear strain rate ($\dot{\epsilon}_{xy}$)
1.5	0.5	0.15	37
2	0.5	0.2	50
2.5	0.5	0.3	75

As is evident from Table 2, shear strain and strain rates increase with increasing speeds. This is along expected lines since deformation mechanisms become more severe when speeds increase. Also evident from the values in Table 2 is that though strains and strain rates are lower than rates typically expected during high-speed machining (due to the cutting speed being low in the present case), the estimates are still higher than those typically associated with those estimated from tensile tests.

6 Conclusions

To characterize how material deforms during machining, this paper discussed the use of a vision-based in-situ monitoring technique that used DIC. Systematic parametric analysis was presented to highlight crucial image and acquisition parameters that affect the noise floor and the estimates of strains and strain rates. We observed that the size of the interrogation window does not adversely affect results, as long as the window selected has sufficient speckle patterns to cross correlate. Based on our observations we also recommend that selection of the strain radius should be based on achieving the best plane fit for the displacements. With respect to estimations of strains, since this depends on the reference frame and the framerate, we infer that a better measure to assess deformation behavior would be strain rates.

From our analysis we found that estimating the shear angle from direct measurements from video is must simpler and easier than the standard and otherwise indirect method of inferring it from the measured cut chip thickness. Moreover, since estimates for the coefficient of friction are observed to decrease with cutting speed, and since strain rates were observed to increase with cutting speed, and since these follow expected trends, our framework provides a blueprint for vision-based in-situ characterization of material deformation during machining processes.

Acknowledgements

This work was supported by the Government of India's Science and Engineering Research Board's Core Research Grant number CRG/2020/001010.

References

1. Guo, Y., Compton, W. D., Chandrasekar, S.: In Situ Analysis of Flow Dynamics and Deformation Fields in Cutting and Sliding of Metals. Proceedings of the Royal Society A 471, 2178 (2015).
2. Denkena, B., Krödel, A., Beblein, S.: A novel approach to determine the velocity dependency of the friction behavior during machining by means of digital particle image velocimetry (DPIV). CIRP Journal of Manufacturing Science and Technology, 32, 81-90 (2021).
3. Berezvai, S., Bachrathy, D., Stepan, G.: High-Speed Camera Measurements in the Mechanical Analysis of Machining. Procedia CIRP 77,155–158 (2018).
4. Thimm, B., Glavas, A., Reuber, M., Christ, H. J.: Determination of chip speed and shear strain rate in primary shear zone using digital image correlation (DIC) in linear-orthogonal cutting experiments. Journal of Materials Processing Technology, 289, 116957 (2021).
5. Gupta, D., Udupa, A., Viswanathan, K.: Evaluating performance metrics in non-homogeneous cutting processes using a random-grid based digital image correlation (DIC) method. Manufacturing Letters, Volume 30, 44-48 (2021).
6. Udupa, A., Vandana, A. S., Saei, M., Gupta, D., Mann, J. B., Viswanathan, K., Sundaram, N. K.: Sinuous plastic flow: Mechanics, microstructural basis, and control. International Journal of Machine Tools and Manufacture, Volume 168, (2021).
7. Molnar, T. G., Berezvai, S., Kiss, A. K., Bachrathy, D., Stepan, G.: Experimental investigation of dynamic chip formation in orthogonal cutting. International Journal of Machine Tools and Manufacture, Volume 145, (2019).
8. Nuhman, A., Singh, A., Lambora, R., Law, M.: Methods to estimate subpixel level small motion from video of vibrating cutting tools. CIRP Journal of Manufacturing Science and Technology, 39, 175-184 (2022).
9. Raizada, V., Rajput H. S., Law M.: Comparative Analysis of Image Processing Schemes to Register Motion from Video of Vibrating Cutting Tools. Procedia CIRP, 121, 85-90 (2024).
10. Raizada, V., Law, M.: Obtaining subpixel level cutting tool displacements from video using a CNN architecture. Manufacturing Technology Today, 22(3), 14–19 (2023).

11. Gupta, P., Rajput, H., Law, M.: Vision-based modal analysis of cutting tools. CIRP Journal of Manufacturing Science and Technology 32: 91-107 (2021).
12. Blaber, J., Adair, B., Antoniou, A.: Ncorr: open-source 2D digital image correlation matlab software. Experimental Mechanics, 55(6), 1105-1122 (2015).
13. Altintas, Y.: Manufacturing automation: metal cutting mechanics, machine tool vibrations, and CNC design. 2nd edn. Cambridge University Press, Cambridge (2012).